Microscopy

DOI: 10.1002/anie.200802376

Subdiffraction-Resolution Fluorescence Imaging with Conventional Fluorescent Probes**

Mike Heilemann, Sebastian van de Linde, Mark Schüttpelz, Robert Kasper, Britta Seefeldt, Anindita Mukherjee, Philip Tinnefeld, and Markus Sauer**

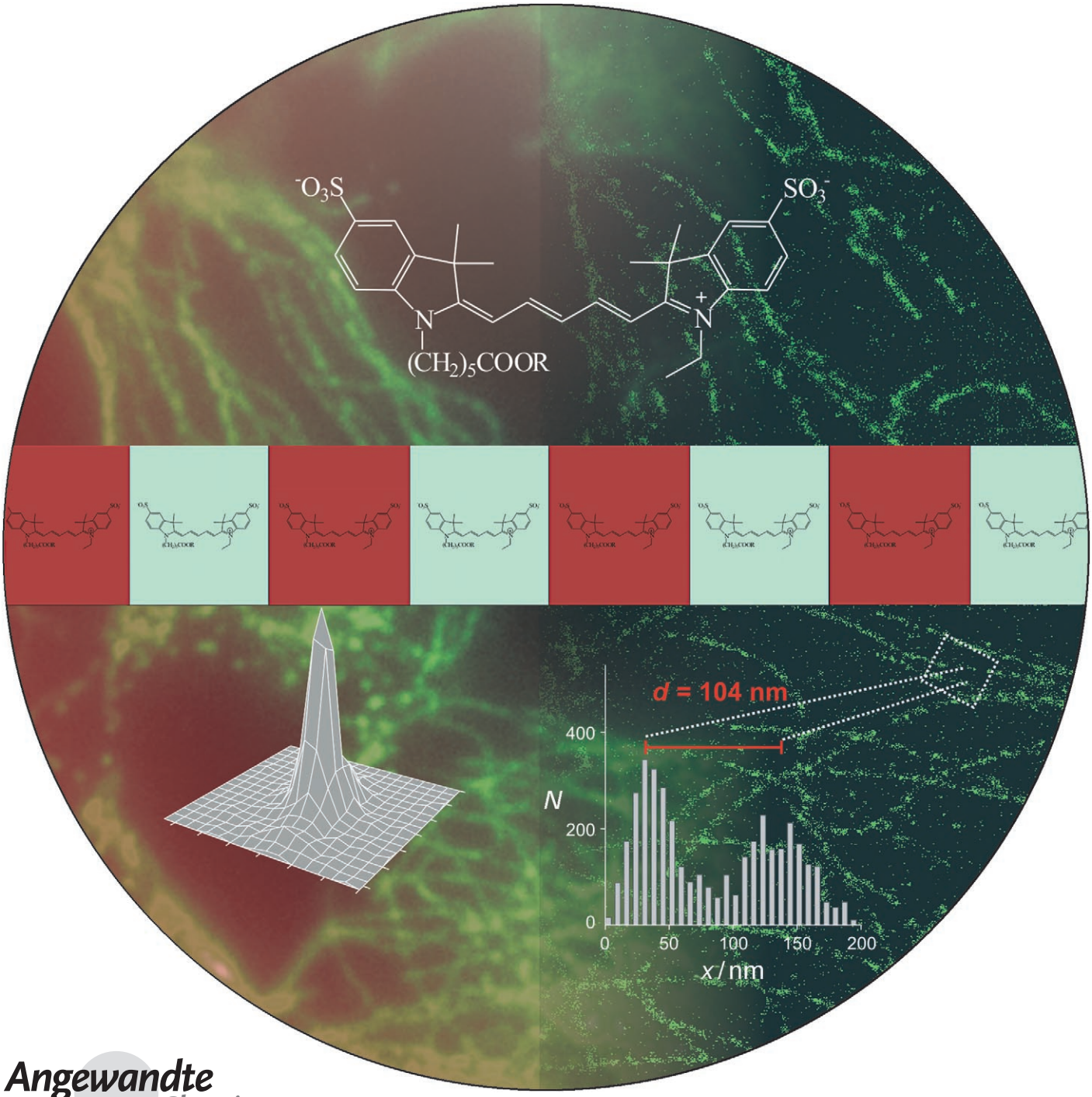

Far-field fluorescence microscopy techniques with increased spatial resolution have the potential to enable a refined understanding of the intracellular organization of cells with near-molecular resolution. In this context, reversibly photoswitchable fluorophores arouse interest as key elements for optical nanoscopy.[1,2] Nonetheless, labeling of intracellular structures with efficient reversibly photoswitchable fluorophores remains challenging. To date, either photoswitchable fluorescent proteins[3] or pairs of fluorophores consisting of a reporter in close proximity to an activator are used.[4]

Herein we show that conventional fluorophores can be used as efficient photoswitchable fluorescent probes. These probes can be reversibly cycled between a fluorescent and a dark state by irradiation with light of different wavelengths without the need for an activator fluorophore.[5] Conceptually analogous to stochastic optical reconstruction microscopy (STORM),[4,6,7] iterative light-induced activation of sparse subsets of fluorophores allows their localization with nanometer accuracy and enables the construction of subdiffraction-resolution images. Because our approach uses conventional cyanine dyes (Cy5, Alexa 647) for cellular staining and does not rely on the proximity of two fluorophores attached to an antibody in a specific ratio and at a specific distance,[4,7] we refer to it as "direct", dSTORM. We demonstrate the potential of dSTORM by subdiffraction-resolution fluorescence imaging of microtubules and actin filaments in mammalian cells with 21-nanometer resolution.

To surpass the diffraction barrier of conventional light microscopy in the axial and lateral directions, different methods have been introduced. These include standing-wave microscopy (SWM)[8] approaches such as 4Pi[9] or wide-field I^5M microscopy[10] and saturated structured-illumination microscopy (SSIM),[11] as well as dynamic concepts such as dynamic saturation optical microscopy (DSOM).[12] Recently, several super-resolution far-field microscopy techniques have been developed that achieve 20- to 30-nm lateral and 50- to 60-nm axial resolution. These include stimulated emission depletion (STED),[1,13–15] STORM,[4,6,7] photoactivated localization microscopy (PALM),[3] and variations thereof.[16–19] While the optical resolution in STED microscopy is improved by efficient de-excitation of the excited singlet state of fluorophores by stimulated emission, the STORM and PALM approaches use reversible saturable optical fluorescence transitions (RESOLFT)[20] between two comparably stable states. These fluorescent and dark states of photoswitchable fluorescent probes can be reversibly transformed into each other upon irradiation with different wavelengths of light with relatively low excitation intensity. Using wide-field fluorescence imaging, fluorophore signals can be detected individually as long as simultaneously emitting molecules are further apart than the minimal distance resolved by the microscope. The position of single fluorophores can then be localized with nanometer accuracy by fitting a two-dimensional Gaussian profile to the individual point-spread function (PSF).[21–25] Ideally, the localization precision depends only on the number of collected photons n and on the standard deviation of the PSF (σ) and can be approximated by $\sigma/\sqrt{n}$.[21] Using efficient reversibly photoswitchable probes, the fluorescence emission profile of individual fluorophores can be modulated in time such that only an optically resolvable subset of fluorophores is activated at any moment.

Inspired by our earlier work on direct photoswitching of cyanine dyes,[5] we show that conventional Cy5 and Alexa 647 fluorophores can be switched reversibly between a fluorescent and dark state with high efficiency (Figure 1a) without the use of an activator fluorophore.[4,6,7,26] This finding enables targeting of intracellular structures with conventional photoswitchable fluorescent probes, for example, commercially available Cy5 or Alexa 647 antibodies, Fab fragments, proteins, peptides, or any other (bio)molecule.

To verify that individual cyanine fluorophores can be switched reversibly between a fluorescent and dark state, Cy5-labeled double-stranded DNA molecules were immobilized on microscope slides and imaged in aqueous buffer (Figure 1a). As shown previously,[5] Cy5 and the structurally very similar cyanine derivative Alexa 647 can be reversibly switched for hundreds of cycles between a fluorescent and dark state without the need of an activator fluorophore. Upon irradiation with red laser light at 647 nm, the fluorophores emit a constant number of photons (typically several thousand per Cy5 molecule)[5,6] and then switch to the dark "off" state with a rate constant k_{off}, which scales linearly with the red laser power (Figure 1b). The activation rate constant k_{on} from the dark to the fluorescent state is also linear with respect to the green laser power (Figure 1c). The required green laser power at 514 nm is about 200 times higher than in methods using an activator fluorophore[4,7] but still stays in the microwatt to milliwatt range. The linear dependence of k_{off} and k_{on} in the lower milliwatt range demonstrates that the switching rates and thus the density of fluorescent probes can be easily controlled by adjusting the red and green laser power.

Fluorescence images were generated by total internal reflection fluorescence (TIRF) microscopy. The samples were simultaneously excited at 647 and 514 nm, and the laser power was adjusted to ensure that only a subset of fluorophores is activated at any time in the field of view. The resulting PSF measured from each activated fluorophore (Figure 1d) was analyzed by fitting a Gaussian function to localize its position with high precision. After thousands of position determina-

[*] Dr. M. Heilemann, S. van de Linde, Dr. M. Schüttpelz, R. Kasper, B. Seefeldt, Dr. A. Mukherjee, Prof. Dr. M. Sauer
Angewandte Laserphysik & Laserspektroskopie
Universität Bielefeld, Universitätsstrasse 25,
33615 Bielefeld (Germany)
Fax: (+49) 521-106-2958
E-mail: heileman@physik.uni-bielefeld.de
sauer@physik.uni-bielefeld.de
Homepage: http://www.physik.uni-bielefeld.de/experi/d3/
Prof. Dr. P. Tinnefeld
Angewandte Physik—Biophysik, and Center for NanoScience
Ludwig-Maximilians-Universität, Amalienstrasse 54,
80799 München (Germany)

[**] The authors thank K. H. Drexhage for stimulating discussion and delivery of Alexa 647–phalloidin and Dr. G. Wiebusch for technical assistance. This work was supported by the Biophotonics program of the German Ministry of Research and Education.

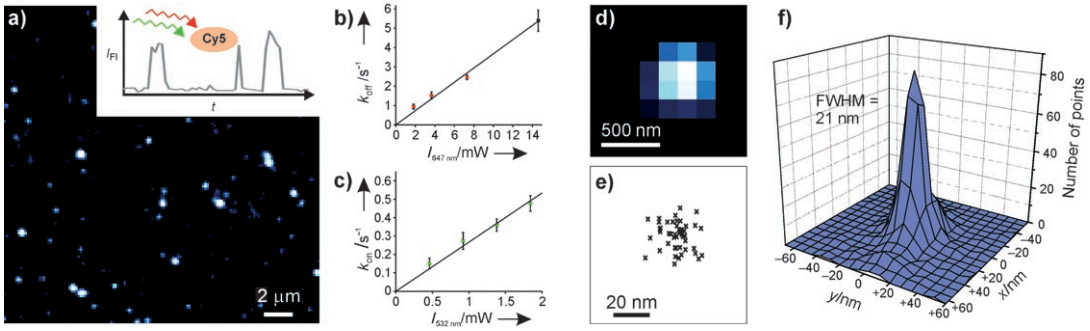

Figure 1. Basic principle of dSTORM using the photoswitchable cyanine dye Cy5. a) TIRF microscope image of Cy5-labeled double-stranded DNA molecules immobilized on microscope slides in aqueous buffer. Upon simultaneous excitation with red (647 nm) and green (514 nm) laser light, Cy5 molecules switch reversibly between a fluorescent "on" and a dark "off" state. b,c) Switching rate constants k_{on} and k_{off} of Cy5 attached to DNA as a function of laser power. d) Conventional fluorescence image showing the typical emission pattern of a single Cy5-labeled DNA molecule. The PSF of activated fluorophores is analyzed by a Gaussian function to determine its precise position. e) Repetitive localizations of a single Cy5-labeled DNA molecule switching between its fluorescent and dark states are represented as crosses. f) Aligned two-dimensional distribution of localizations from 50 Cy5–DNA molecules demonstrates a spatial resolution of 21 ± 1 nm with conventional fluorescent probes.

tions (referred to as localizations),[7] the dSTORM image was reconstructed. The cluster of localizations shown in Figure 1 e results from repetitive localization of a single Cy5-labeled DNA molecule switching between the fluorescent and the dark state. By aligning the localizations from several clusters, a histogram was generated and fitted by a Gaussian function to yield a full width at half maximum of 21 ± 1 nm (Figure 1 f). This result suggests a resolution of approximately 20 nm for fluorescence imaging with conventional fluorescent probes.

The application of dSTORM for intracellular subdiffraction-resolution fluorescence imaging of filamentous cytoskeleton structures is shown in Figures 2 and 3. For immunofluorescence imaging of microtubules, mammalian COS-7 cells were stained with primary antibodies and then with commercially available Alexa-647-labeled Fab fragments. Reconstructed images of microtubules were obtained by direct iterative stochastic activation of subsets of Alexa 647 molecules and subsequent position determinations applying simultaneous excitation at 514 and 647 nm. Typically, we recorded 5000–40 000 frames at frame rates of 5–40 Hz, resulting in acquisition times of approximately eight minutes for a total image. During this time, no mechanical stabilization or drift correction was necessary.

As can be seen in Figure 2, the dSTORM images show better resolution than conventional wide-field epifluorescence images of the microtubule network. The improvement in spatial resolution achieved with dSTORM is demonstrated with single microtubule filaments (Figure 2 c, e). From cross-sectional profiles (Figure 2 f, g), we measure apparent widths of individual microtubule filaments of 35–50 nm. Compared to previous studies, this value is somewhat closer to the actual diameter expected for a single microtubule filament of approximately 25 nm,[27] because dSTORM can use smaller singly labeled Fab fragments instead of a set of primary antibodies and multiple labeled secondary antibodies.[7] Thus, the use of smaller fluorescent probes in dSTORM improves the intrinsic imaging resolution. Furthermore, commercially available fluorescently labeled primary antibodies, Fab fragments, or even smaller peptide tags can be directly applied for subdiffraction-resolution fluorescence imaging of intracellular structures.

This ability is exemplified using the fluorescent probe Alexa 647–phallodin, a bicyclic heptapeptide that binds to actin filaments (Figure 3). G-actin fibers were polymerized on glass substrate. The dSTORM image visualizes single F-actin fibers, in contrast to the conventional fluorescence image (Figure 3 a, b). F-actin filaments play a central role in various types of motility, including muscle contraction and transport processes. In vivo, F-actin rarely exists as isolated single filaments with a diameter of approximately 7 nm but instead associates into bundles in which specific proteins separate individual filaments by approximately 35 nm.[28] The dSTORM images show a drastic improvement in the resolution of F-actin filaments as compared to the conventional fluorescence image (Figure 3 c–e). In some densely packed regions, filament bundles separated by less than 100 nm with a diameter of approximately 100 nm (FWHM) are clearly resolved in cross-sectional profiles (Figure 3 f). These dSTORM results agree quantitatively with the size distribution determined by other alternative methods.[29] Moreover, the cross-sectional profiles of filament bundles indicate the existence of smaller substructures, as expected for individual filaments separated by several tens of nanometers.

In summary, we introduce a new and very simple activator-free method for subdiffraction-resolution fluorescence imaging based on the photoswitching of standard organic fluorophores. Our dSTORM method enables the use of small, singly labeled, and commercially available fluorescent probes for the specific labeling and imaging of intracellular structures with approximately 20-nm resolution within minutes and circumvents the complicated double labeling of antibodies with activator–reporter pairs in a specific ratio and at a given distance. Furthermore, the method can easily be combined with protein tags, such as the SNAP tag, to specifically label target proteins in cells.[30] Since other spectrally different cyanine dyes such as Cy5.5, Cy7, or

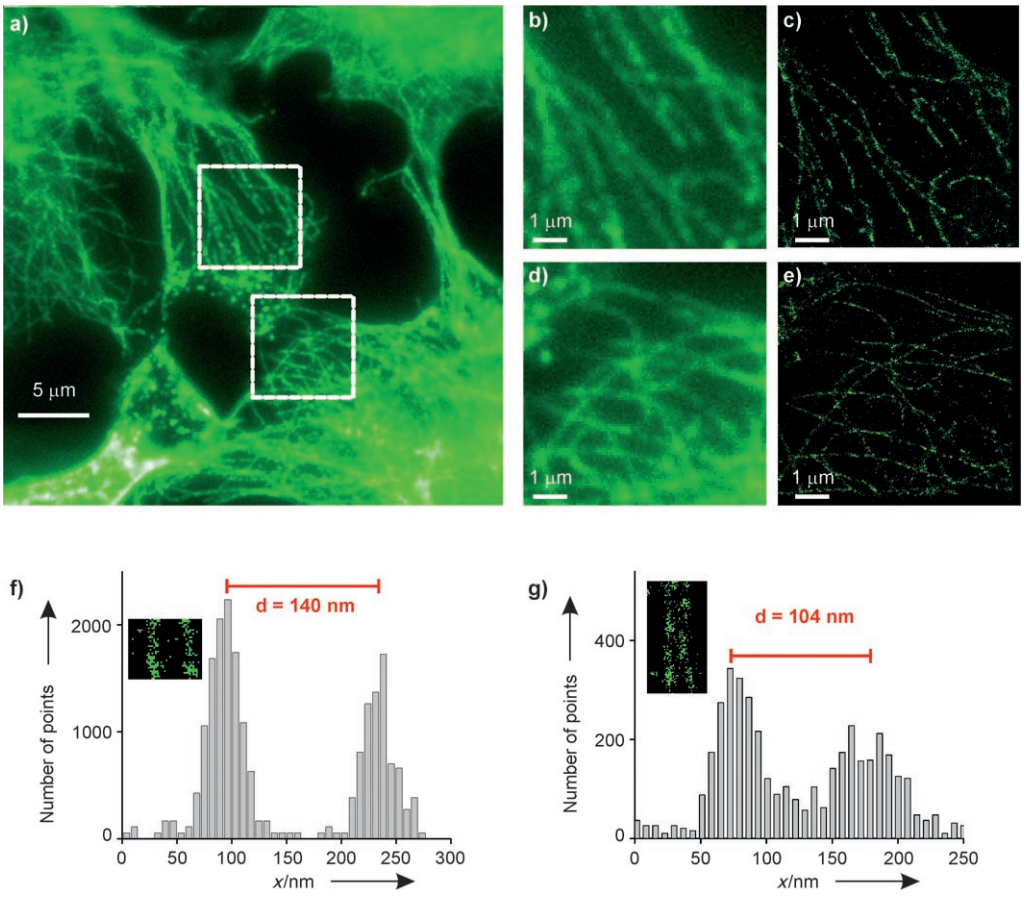

Figure 2. dSTORM imaging of microtubules in mammalian cells. a) Immunofluorescence image of microtubules in COS-7 cells labeled with a primary antibody and Alexa 647 Fab fragments. b,d) Conventional and c,e) dSTORM images of boxed regions in (a). f,g) Cross-sectional profiles of adjacent microtubule filaments arranged 140 and 104 nm apart in the cell. The insets show the corresponding dSTORM images.

Alexa 680 can also be switched reversibly between a fluorescent and a dark state,[7] dSTORM can also be extended to multicolor subdiffraction-resolution fluorescence imaging.

Experimental Section

To study switching characteristics of the carbocyanine dye Cy5 in the absence and presence of the activator dye Cy3, a 43-base-pair single-stranded DNA was used in which Cy5 and the activator Cy3 were separated by nine base pairs.[4,7] Complementary strands of DNA were annealed to form biotinylated double-stranded DNA (dsDNA) by mixing equimolar amounts of the two complementary strands in 10 mM Tris–HCl (pH 7.5) containing 50 mM NaCl (Tris = tris(hydroxymethyl)aminomethane). The dsDNA was immobilized on streptavidin-coated glass slides (LabTek, Nunc).[4] The chambers were sealed by a silicon gasket. Single-molecule imaging was performed in "switching buffer": phosphate-buffered saline (PBS, pH 7.4), containing oxygen scavenger (0.5 mg mL^{-1} glucose oxidase (Sigma), 40 μg mL^{-1} catalase (Roche Applied Science), 10% w/v glucose) and 50 mM β-mercaptoethylamine (MEA).

To measure switching kinetics, the DNA samples were first irradiated at 647 nm to switch Cy5 into the dark state. The rate constant k_{off} at which Cy5-labeled DNA switches into the dark state was calculated by fitting the number of fluorescent molecules upon irradiation at 647 nm as a function of time to a single exponential function. As

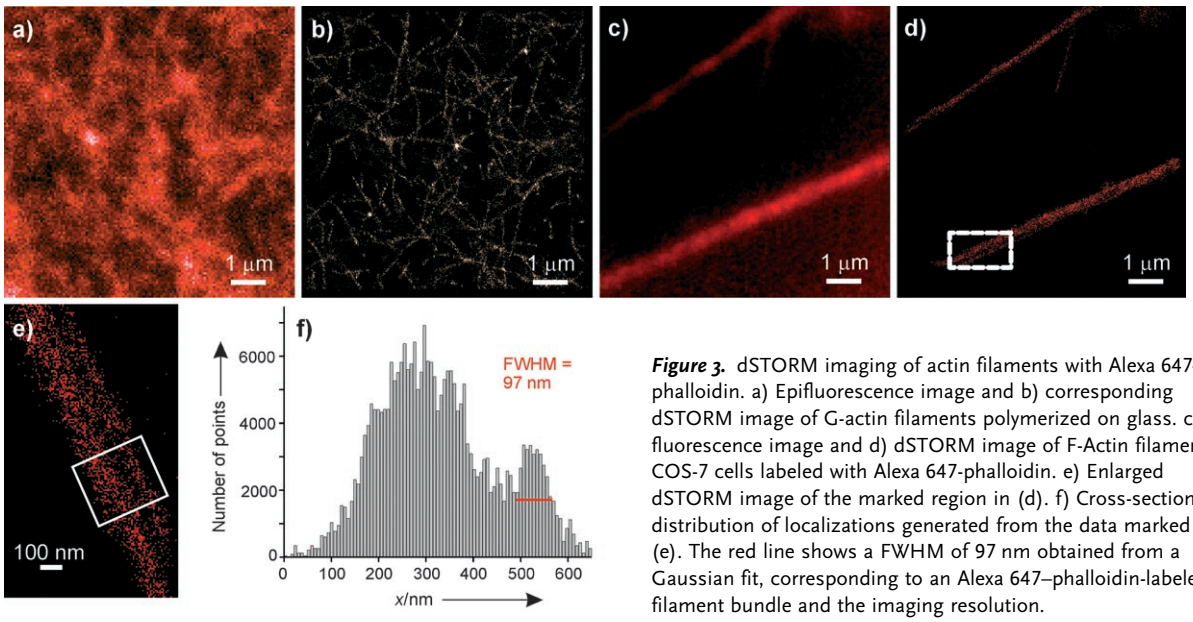

Figure 3. dSTORM imaging of actin filaments with Alexa 647–phalloidin. a) Epifluorescence image and b) corresponding dSTORM image of G-actin filaments polymerized on glass. c) Epifluorescence image and d) dSTORM image of F-Actin filaments in COS-7 cells labeled with Alexa 647-phalloidin. e) Enlarged dSTORM image of the marked region in (d). f) Cross-sectional distribution of localizations generated from the data marked in (e). The red line shows a FWHM of 97 nm obtained from a Gaussian fit, corresponding to an Alexa 647–phalloidin-labeled filament bundle and the imaging resolution.

expected, k_{off} was independent of the absence or presence of the activator. The reactivation with rate constant k_{on} in the absence and presence of the activator Cy3 was determined by irradiating the sample at 514 nm while the red imaging laser (647 nm) remained on. Thus, the number of active (fluorescent) fluorophores reached an equilibrium between activation and deactivation. The number of fluorophores in the active state at equilibrium was measured, and k_{on} was then calculated from k_{off} and the fraction of fluorophores in the active state at equilibrium according to the relation $M_{active}/M_{total} = k_{on}/(k_{on}+k_{off})$.

African green monkey kidney COS-7 cells were plated in LabTek 8-well chambered coverglass (Nunc). After 12–24 h, the cells were fixed using 3.7% paraformaldehyde in PBS for 10 min. The fixed cells were washed five times with PBS and permeabilized in blocking buffer (PBS containing 5% w/v normal goat serum (NGS; Sigma) and 0.5% v/v Triton X-100) for 15 min. F-actin was stained by incubation with Alexa 647–phalloidin (10^{-6}–10^{-7} M, provided by K. H. Drexhage, University of Siegen) for 30 min and washed three times using PBS containing 0.1% v/v Tween 20 (Sigma). Microtubules were stained with mouse monoclonal anti-β-tubulin antibodies (clone: 2-28-33, Invitrogen) for 30 min and then with Alexa-647-labeled goat anti-mouse $F(ab')_2$ fragments (Invitrogen) serving as secondary antibody, also for 30 min. The labeling stoichiometry of $F(ab')_2$ fragments was characterized to be approximately two. Three washing steps using PBS containing 0.1% v/v Tween 20 were performed after each staining step. Before dSTORM imaging, the PBS buffer was replaced by switching buffer.

G-actin monomers from bovine muscle (Sigma, 5 μM) were polymerized in untreated LabTek chambers in the presence of 10 mM imidazole·HCl at pH 7.2, 100 mM KCl, 2 mM $MgCl_2$, and 1 mM ATP. Subsequently, the surface was incubated with Alexa 647–phalloidin (10^{-5}–10^{-7} M) for 60–120 min and washed three times using PBS containing 0.1% v/v Tween 20.

Fluorescence imaging was performed on an Olympus IX-71 applying an objective-type total internal reflection fluorescence (TIRF) configuration using an oil-immersion objective (PlanApo 60x, NA 1.45, Olympus). Two continuous-wave laser beams of an argon–krypton laser (Innova 70C, Coherent) were selected by an acousto-optic tunable filter (AOTF) and used simultaneously for readout and activation. The laser beams were coupled into the microscope objective by a polychromic beamsplitter (532/647, AHF Analysentechnik). Fluorescence light was spectrally filtered with two filters (700DF75 and HQ542LP, AHF Analysentechnik) and imaged on an EMCCD camera (Andor Ixon DV897DCS-BV). Additional lenses were used to achieve a final imaging magnification of 100 to 225 times, that is, a pixel size from 160 to 70 nm. Typical laser powers used for dSTORM imaging were 0.25 mW (514 nm) and 15 mW (647 nm). The laser powers were chosen to ensure that the fraction of activated fluorophores at any given time was sufficiently low to allow the recognition of individual fluorophores. Typically, we recorded 5000–40000 frames at frame rates of 5–40 Hz. Applying a laser power of 15 mW at 647 nm, we detected 300–500 photons in 50 ms per molecule, corresponding to an average precision of single-molecule localization of 15–20 nm.[21] Under these imaging conditions, an average fluorophore remains in the active state for several frames after activation, resulting in several thousand photons detected per molecule and switching cycle.

Fluorescent spots identified in each image frame were fit to a Gaussian function to determine their center of mass. Spots appearing too dim, too wide, or too elliptical were discarded from further analysis.[7] For image reconstruction, each actual pixel was partitioned into ten subpixels, resulting in a pixel size from 16 to 7 nm, and each center of mass calculated from individual fluorophores was assigned to a particular subpixel. The brightness is determined by the number of localizations falling into a subpixel.

Received: May 21, 2008
Published online: July 22, 2008

Keywords: fluorescent probes · imaging agents · localization microscopy · optical switches · subdiffraction resolution

[1] S. W. Hell, *Science* **2007**, *316*, 1153.
[2] M. Sauer, *Proc. Natl. Acad. Sci. USA* **2005**, *102*, 9433.
[3] E. Betzig, G. H. Patterson, R. Sougrat, O. W. Lindwasser, S. Olenych, J. S. Bonifacino, M. W. Davidson, J. Lippincott-Schwartz, H. F. Hess, *Science* **2006**, *313*, 1642.
[4] B. Huang, W. Wang, M. Bates, X. Zhuang, *Science* **2008**, *319*, 810.
[5] M. Heilemann, E. Margeat, R. Kasper, M. Sauer, P. Tinnefeld, *J. Am. Chem. Soc.* **2005**, *127*, 3801.
[6] M. J. Rust, M. Bates, X. Zhuang, *Nat. Methods* **2006**, *3*, 793.
[7] M. Bates, B. Huang, G. T. Dempsey, X. Zhuang, *Science* **2007**, *317*, 1749.
[8] B. Bailey, D. L. Farkas, D. L. Taylor, F. Lanni, *Nature* **1993**, *366*, 44.
[9] S. W. Hell, E. H. K. Stelzer, *Opt. Commun.* **1992**, *93*, 277.
[10] M. G. Gustafsson, D. A. Agard, J. W. Sedat, *J. Microsc.* **1999**, *195*, 10.
[11] M. G. Gustafsson, *Proc. Natl. Acad. Sci. USA* **2005**, *102*, 133081.
[12] J. Enderlein, *Appl. Phys. Lett.* **2005**, *87*, 095105.
[13] S. W. Hell, J. Wichmann, *Opt. Lett.* **1994**, *19*, 780.
[14] V. Westphal, S. O. Rizzoli, M. A. Lauterbach, D. Kamin, R. Jahn, S. W. Hell, *Science* **2008**, *320*, 246.
[15] K. I. Willig, S. O. Rizzoli, V. Westphal, R. Jahn, S. W. Hell, *Nature* **2006**, *440*, 935.
[16] S. T. Hess, T. P. K. Girirajan, M. D. Mason, *Biophys. J.* **2006**, *91*, 4258.
[17] A. Egner, C. Geisler, C. von Middendorff, H. Bock, D. Wenzel, R. Medda, M. Andresen, A. C. Stiel, S. Jakobs, C. Eggeling, A. Schönle, S. W. Hell, *Biophys. J.* **2007**, *93*, 3285.
[18] C. Flors, J. Hotta, H. Uji-i, P. Dedecker, R. Ando, H. Mizuno, A. Miyawaki, J. Hofkens, *J. Am. Chem. Soc.* **2007**, *129*, 13970.
[19] H. Bock, C. Geisler, C. A. Wurm, C. von Middendorff, S. Jakobs, A. Schönle, A. Egner, S. W. Hell, C. Eggeling, *Appl. Phys. B* **2007**, *88*, 161.
[20] S. W. Hell, *Nat. Biotechnol.* **2003**, *21*, 1347.
[21] R. E. Thompson, D. R. Karson, W. W. Webb, *Biophys. J.* **2002**, *82*, 2775.
[22] A. Yildiz, J. N. Forkey, S. A. McKinney, T. Ha, Y. E. Goldman, P. Selvin, *Science* **2003**, *300*, 2061.
[23] K. A. Lidke, B. Rieger, T. M. Jovin, R. Heintzmann, *Opt. Express* **2005**, *13*, 7052.
[24] A. Sharonov, R. M. Hochstrasser, *Proc. Natl. Acad. Sci. USA* **2006**, *103*, 18911.
[25] S. Ram, E. S. Ward, R. J. Ober, *Proc. Natl. Acad. Sci. USA* **2006**, *103*, 4457.
[26] M. Bates, T. R. Blosser, X. Zhuang, *Phys. Rev. Lett.* **2005**, *94*, 108101.
[27] K. Weber, P. C. Rathke, M. Osborn, *Proc. Natl. Acad. Sci. USA* **1978**, *75*, 1820.
[28] J. Vandekerckhove, K. Weber, *J. Mol. Biol.* **1978**, *126*, 783.
[29] E. Chung, D. Kim, Y. Cui, Y.-H. Kim, P. T. C. So, *Biophys. J.* **2007**, *93*, 1747.
[30] N. Johnsson, K. Johnsson, *ACS Chem. Biol.* **2007**, *2*, 31.

